Acta Biomaterialia xxx (2015) xxx–xxx

Contents lists available at ScienceDirect

Acta Biomaterialia

journal homepage: www.elsevier.com/locate/actabiomat

A novel bioreactor for the generation of highly aligned 3D skeletal muscle-like constructs through orientation of fibrin via application of static strain

Philipp Heher [a,b,c,*,1], Babette Maleiner [b,d,1], Johanna Prüller [a,b,d,1], Andreas Herbert Teuschl [b,d,e], Josef Kollmitzer [d,f], Xavier Monforte [b,d], Susanne Wolbank [a,b,c], Heinz Redl [a,b,c], Dominik Rünzler [b,d], Christiane Fuchs [b,d,e]

[a] Trauma Care Consult, Vienna, Austria
[b] Austrian Cluster for Tissue Regeneration, Vienna, Austria
[c] Ludwig Boltzmann Institute for Experimental and Clinical Traumatology/AUVA Research Center, Vienna, Austria
[d] Department of Biochemical Engineering, UAS Technikum Wien, Vienna, Austria
[e] City of Vienna Competence Team Bioreactors, UAS Technikum Wien, Vienna, Austria
[f] Higher Technical Institute HTL –TGM, Department for Biomedical- and Health-Engineering, Vienna, Austria

ARTICLE INFO

Article history:
Received 11 March 2015
Received in revised form 10 June 2015
Accepted 29 June 2015
Available online xxxx

Keywords:
Skeletal muscle
Tissue engineering
Mechanical stimulation
Bioreactor
Fibrin

ABSTRACT

The generation of functional biomimetic skeletal muscle constructs is still one of the fundamental challenges in skeletal muscle tissue engineering. With the notion that structure strongly dictates functional capabilities, a myriad of cell types, scaffold materials and stimulation strategies have been combined. To further optimize muscle engineered constructs, we have developed a novel bioreactor system (MagneTissue) for rapid engineering of skeletal muscle-like constructs with the aim to resemble native muscle in terms of structure, gene expression profile and maturity.

Myoblasts embedded in fibrin, a natural hydrogel that serves as extracellular matrix, are subjected to mechanical stimulation via magnetic force transmission. We identify static mechanical strain as a trigger for cellular alignment concomitant with the orientation of the scaffold into highly organized fibrin fibrils. This ultimately yields myotubes with a more mature phenotype in terms of sarcomeric patterning, diameter and length. On the molecular level, a faster progression of the myogenic gene expression program is evident as myogenic determination markers *MyoD* and *Myogenin* as well as the Ca^{2+} dependent contractile structural marker *TnnT1* are significantly upregulated when strain is applied.

The major advantage of the MagneTissue bioreactor system is that the generated tension is not exclusively relying on the strain generated by the cells themselves in response to scaffold anchoring but its ability to subject the constructs to individually adjustable strain protocols. In future work, this will allow applying mechanical stimulation with different strain regimes in the maturation process of tissue engineered constructs and elucidating the role of mechanotransduction in myogenesis.

Statement of Significance

Mechanical stimulation of tissue engineered skeletal muscle constructs is a promising approach to increase tissue functionality. We have developed a novel bioreactor-based 3D culture system, giving the user the possibility to apply different strain regimes like static, cyclic or ramp strain to myogenic precursor cells embedded in a fibrin scaffold. Application of static mechanical strain leads to alignment of fibrin fibrils along the axis of strain and concomitantly to highly aligned myotube formation. Additionally, the pattern of myogenic gene expression follows the temporal progression observed *in vivo* with a more thorough induction of the myogenic program when static strain is applied. Ultimately, the strain protocol used in this study results in a higher degree of muscle maturity demonstrated by enhanced sarcomeric patterning and increased myotube diameter and length. The introduced

* Corresponding author at: Trauma Care Consult, Gonzagagasse 11/25, 1010 Vienna, Austria.
E-mail address: heherp@technikum-wien.at (P. Heher).
[1] These authors contributed equally to this work.

http://dx.doi.org/10.1016/j.actbio.2015.06.033
1742-7061/

bioreactor system enables new possibilities in muscle tissue engineering as longer cultivation periods and different strain applications will yield tissue engineered muscle-like constructs with improved characteristics in regard to functionality and biomimicry.

1. Introduction

Skeletal muscle is the most abundant tissue type in the human body, accounting for roughly 40% of the total body mass [1]. Despite recent advances in the treatment of damaged skeletal muscle tissue clinical outcomes have been at best suboptimal [2,3]. In this respect, tissue engineering of transplantable functional skeletal muscle serves as an attractive alternative to replace and/or restore the damaged tissue. To achieve this goal, a variety of two- and three-dimensional skeletal muscle tissue engineering strategies have been developed, utilizing diverse scaffold materials and cell types [3–5]. Ever since Vandenburgh et al.'s pioneering work on myotube formation in collagen gels [6,7], natural hydrogels have been extensively used as scaffold materials for skeletal muscle engineering due to their biocompatibility and -degradability [8–14]. Compared to non-biodegradable or synthetic materials, fibrin hydrogels offer superior properties for 3D skeletal muscle engineering [3], as they mimic the mechanical properties of native skeletal muscle tissue, with the possibility to modulate stiffness and pore size [15–17]. Moreover, they allow for dense and spatially uniform cell distribution due to the high abundance of cell attachment sites – a crucial feature as the cell seeding density has been shown to directly affect myogenic differentiation and muscle structure [18,19]. Besides, fibrin hydrogels have the advantage of binding growth factors that augment myogenesis, such as vascular endothelial growth factor (VEGF) [20], basic fibroblast growth factor-2 (bFGF-2) [21,22] or, indirectly, insulin-like growth factor-1 (IGF-1) [23]. Altogether, these features render fibrin a very promising scaffold material for skeletal muscle engineering approaches.

From a developmental point of view, the functional capabilities of skeletal muscle tissue are strongly linked to its structure [24]. In general, skeletal muscle is characterized by a highly ordered array of parallel muscle fibers. These initially originate from the fusion of myogenic precursor cells into multi-nucleated myotubes which later mature into muscle fibers comprised of many parallel myofibrils [5]. This maturation is accompanied by an increase in contractile force of the myofibril, which is actuated through relative movement of two interlocking macrostructures (myofilaments), the thin actin and thick myosin filaments [25]. As the main purpose of skeletal muscle tissue is to generate uniaxial force, engineered muscle constructs are expected to generate sufficiently large contractile forces to be able to restore the impaired host muscle function upon transplantation. Thus, two fundamental goals in skeletal muscle tissue engineering are parallel alignment of myotubes and a high degree of muscle maturity. With the notion that mechanotransduction plays a central role in myogenic differentiation [26], mechanical stimulation has been demonstrated to induce cellular alignment along the axis of strain [6,9] and to stimulate muscle growth *in vitro* and *in vivo* [27,28]. While static mechanical stimulation is largely considered a trait related to induction of myogenic differentiation, inconsistent findings have been reported regarding the role of cyclic mechanical stimulation on signaling and myogenic marker expression, respectively [29–32].

For the generation of engineered biomimetic muscle constructs several strategies have been proposed. With regard to cellular alignment, micropatterned polymer surfaces offering precise control over scaffold nano- or microtopology have been used to promote guided myotube formation [33–35]. In terms of muscle maturity, electric stimulation has been demonstrated to enhance the contractile force of engineered muscle in two- and three-dimensional settings [36–39]. In the past, diverse bioreactor systems enabling mechanical stimulation of cell-seeded scaffolds have been developed, serving as platforms that promote myotube alignment as well as muscle maturation. In an elegant approach, many of these systems make use of the contractile force that muscle cells generate upon differentiation: fixation of a scaffold between two anchor points creates predictable lines of isometric strain as the cells pull against the stationary posts. This cell-mediated internal tension has been shown to be sufficient to promote alignment along the principle axis of strain [9,10,40]. The majority of previously reported 3D skeletal muscle engineering approaches use scaffold anchoring as the primary source of strain to generate alignment, with the limitation that the extent and type of strain cannot be properly controlled. With the notion that provision of defined mechanical stimuli plays a central role in myogenesis, recent efforts in skeletal muscle engineering have focused on the development of bioreactors that allow for tunable mechanical stimulation [9,11,27,41]. To generate biomimetic skeletal muscle constructs applying a physiologically relevant strain regime, we have designed a novel closed bioreactor system (MagneTissue) that allows for adjustable cyclic or static mechanical stimulation of cells embedded in a free standing ring-shaped fibrin matrix via strain transmission through magnetic force. With this system we sought to analyze the effect of a defined repetitive static stimulation protocol on cell alignment, morphology, myogenic differentiation and maturation of myotubes. Furthermore, we wanted to test whether application of static strain improves the myogenic outcome to a higher extent than scaffold anchoring. We demonstrate that, over a culture period of 9 days, static mechanical stimulation facilitates myoblast differentiation into a highly organized array of myotubes with widespread sarcomeric patterning and increased diameter compared to non-stimulated constructs. Moreover, we show that myogenic marker gene expression is enhanced when static strain is applied and generally follows a temporal physiological pattern, which demonstrates the high performance of the MagneTissue bioreactor system as a novel organotypic *in vitro* model for skeletal muscle tissue engineering.

2. Materials and methods

If not indicated otherwise, all chemicals and reagents were purchased from Sigma Aldrich (Vienna, Austria) and were of analytical grade. Primary antibodies for immunofluorescence stainings were anti-Myosin heavy chain (MHC) recognizing all MHC fast isoforms (Sigma Aldrich, Vienna, Austria) and anti-Desmin (Cell Signaling, Cambridge, United Kingdom). Secondary antibodies labelled with Alexa Fluor 488 were purchased from Life Technologies (Lofer, Austria).

2.1. Cell culture

The mouse myoblast cell line C2C12 (American Type Culture Collection, Manassas, USA) was cultured in Dulbecco's modified Eagle's medium high Glucose (DMEM-HG; Life Technologies,

Please cite this article in press as: P. Heher et al., A novel bioreactor for the generation of highly aligned 3D skeletal muscle-like constructs through orientation of fibrin via application of static strain, Acta Biomater. (2015), http://dx.doi.org/10.1016/j.actbio.2015.06.033

Carlsbad, California), supplemented with 10% fetal calf serum (FCS; GE Healthcare, Buckinghamshire, United Kingdom), 1% penicillin/streptomycin (P/S; Lonza, Basel Switzerland) and 1% L-glutamine (Lonza, Basel Switzerland). This medium will be referred to as growth medium (GM). Cells were grown on standard cell culture dishes (Starlab, Hamburg, Germany) in a humidified incubator at 37 °C and 5% CO_2 and subcultured at 70–80% confluency to avoid induction of differentiation. Differentiation was induced by exchanging GM with DMEM-HG supplemented with 3% horse serum, 1% P/S and 1% L-glutamine, referred to as differentiation medium (DM). Both GM and DM were supplemented with the fibrinolysis inhibitor aprotinin (Baxter, Deerfield, USA) at a final concentration of 100 KIU/mL for culture of cells in fibrin scaffolds. For 2D plastic control (cells cultured on standard cell culture dishes) and 2D fibrin control (cells cultured on top of a fibrin matrix; Fig. 4A and B, respectively) differentiation experiments, the same cell seeding densities (5×10^5 cells per well in a 6-well plate) were used. Furthermore, the same fibrin composition was used (20 mg/mL fibrinogen and 0.625 U/mL thrombin) for 2D culture and, subsequently, for the generation of the 3D fibrin constructs with embedded C2C12 mouse myoblasts.

2.2. Preparation and culture of fibrin rings

The clinically approved Tissucol Duo 500 5.0 ml Fibrin Sealant (Baxter, Illinois, USA) was used for preparation of the fibrin scaffolds. The scaffold molds (6 rings per mold) used to cast ring-shaped scaffolds (2 mm in diameter and 3 cm in length) were custom-made from either polyoxymethylene (POM) or stainless steel coated with Teflon (Fig. 1A). Fibrinogen was diluted to a concentration of 40 mg/mL with GM. Thrombin, diluted to 4 U/mL with 40 mmol/L $CaCl_2$, was homogeneously mixed with C2C12 cells in GM to a final concentration of 1.25 U/mL thrombin. 0.5 mL of the thrombin/cell suspension were mixed with 0.5 mL fibrinogen/GM solution and two scaffolds were cast immediately. The final concentrations for each scaffold were: 20 mg/mL fibrinogen, 0.625 U/mL thrombin and 3.2×10^6 cells per scaffold (corresponding to 6.4×10^6 cells/mL). After casting, the scaffolds were left to polymerize at 37 °C and 5% CO_2 for 45 min. Fibrin rings of the unstrained or strained group were mounted onto a custom-made spool-hook system (Fig. 1B). All scaffolds were cultivated in 14 mL Snap-Cap Falcon tubes (BD Biosciences, Bedford, USA). Scaffolds were either kept floating in medium (control group; Fig. 1C) or were mounted onto the spool-hook system and stored in custom-made magnetic racks to keep them at 0% strain, representing the unstrained control group (Fig. 1D). The same racks were used for the strain group until day 3 before they were applied to the MagneTissue bioreactor system for mechanical stimulation (Fig. 1E).

2.3. MagneTissue bioreactor system

The MagneTissue system is designed to fit into common cell incubators to guarantee a culture environment of 37 °C and 5% CO_2. The bioreactor system has two superimposed rows holding the samples (Fig. 1E and F). Each row consists of a top sample holder plate which carries three tube cassettes for 6 samples each (36 samples in total) and a bottom plate containing permanent magnets which interact with the permanent magnets integrated into the hooks. By driving the bottom plate with a stepper motor the position of the hook is controlled contactless via magnetic force transmission. As a consequence, the relative movement of the bottom plate to the fixed top sample holder plate results in straining and/or relaxation of the fibrin samples. The mechanical part of the bioreactor system consists of a stepper motor which is mounted on an aluminum strut profile vertically to the bottom plate of the framework. The motor is integrated into a low profile linear axis (DryLin® SLN, igus GmbH, Cologne, Germany) in which it drives a ball-bearing spindle with a maximum driving torque of 0.1 Nm. To minimize torsion as a result of the applied movement a linear slide is mounted opposite to the motor linear axis. To control the movements of the stepper motor, controlled via the microcontroller ATmega16U2 (Atmel, San José, USA), an operator interface was programmed using MATLAB (The MathWorks GmbH, Ismaning, Germany). This software provides independent control of translational movements which can be set in mm up to resolutions of 10 μm. Furthermore, it allows the user to run cyclic motion patterns in number of cycles/min for the duration of an experiment. With the current set-up, movement speeds of 4 mm/s can be realized. Hardware components for power supply and necessary modules for the motion control of the stepper motors are combined in a cubicle of electronic equipment.

2.4. Mechanical characterization of fibrin scaffolds

Tensile tests were performed using a Zwick BZ2.5/TN1S uniaxial material testing machine (Zwick GmbH & Co. KG, Ulm, Germany) with a 50 N load cell. Prior to testing, the scaffolds were equilibrated in 1x PBS for 24 h and subsequently mounted on two spools – the same as used in the bioreactor system – for measurements. Samples were strained to failure at a rate of 20 mm/min at room temperature and a relative humidity of 45–65%. Data was recorded after achieving a pre-load of 10 mN. To calculate the Young's modulus, the linear portion of the stress/strain curve was used. Maximum clot firmness (MCF) was determined with rotational thromboelastometry (ROTEM) using a ROTEM© delta thromboelastometry system (TEM Innovations GmbH, Munich, Germany). Briefly, 300 μl of each fibrin formulation were used per measurement and the MCF was calculated live with the integrated ROTEM© delta software (build 1.6.0).

2.5. Mechanical stimulation of fibrin rings

At day 3 of culture mechanical stimulation in the MagneTissue bioreactor system was started by application of 10% static strain for 6 h followed by an 18 h rest phase at 3% static strain (Fig. 1G). This strain protocol was repeated for 6 days (including day 9). Furthermore, myogenic differentiation was induced by exchanging GM with DM supplemented with 100 KIU/mL aprotinin for 24 h. From day 4 on, the media was partially changed every second day with GM supplemented with 100 KIU/mL aprotinin (5 mL new + 4 mL old medium).

2.6. Live/dead staining

At day 0, 3, 6 and 9 after scaffold preparation cell viability was assessed by staining the cells with Calcein AM and propidium iodide (PI). Whole fibrin rings were stained in serum free DMEM-HG medium containing 2.5 μg/mL Calcein AM and 1 μg/mL PI for 30 min at 37 °C in the dark. The rings were analyzed with a Leica DMI6000B epifluorescence microscope (Leica Microsystems GmbH, Wetzlar, Germany).

2.7. Immunohistochemistry

Samples were fixed with 4% paraformaldehyde (PFA; Roth, Karlsruhe, Germany) for a maximum of 24 h at 4 °C. For immunofluorescence staining, the samples were permeabilized with Tris-Buffered Saline/0.1% (v/v) Triton X-100 (TBS/T), followed by a blocking step for 1 h in PBS/T-1% (w/v) bovine serum albumin (BSA) at room temperature. Subsequently, the samples were

Please cite this article in press as: P. Heher et al., A novel bioreactor for the generation of highly aligned 3D skeletal muscle-like constructs through orientation of fibrin via application of static strain, Acta Biomater. (2015), http://dx.doi.org/10.1016/j.actbio.2015.06.033

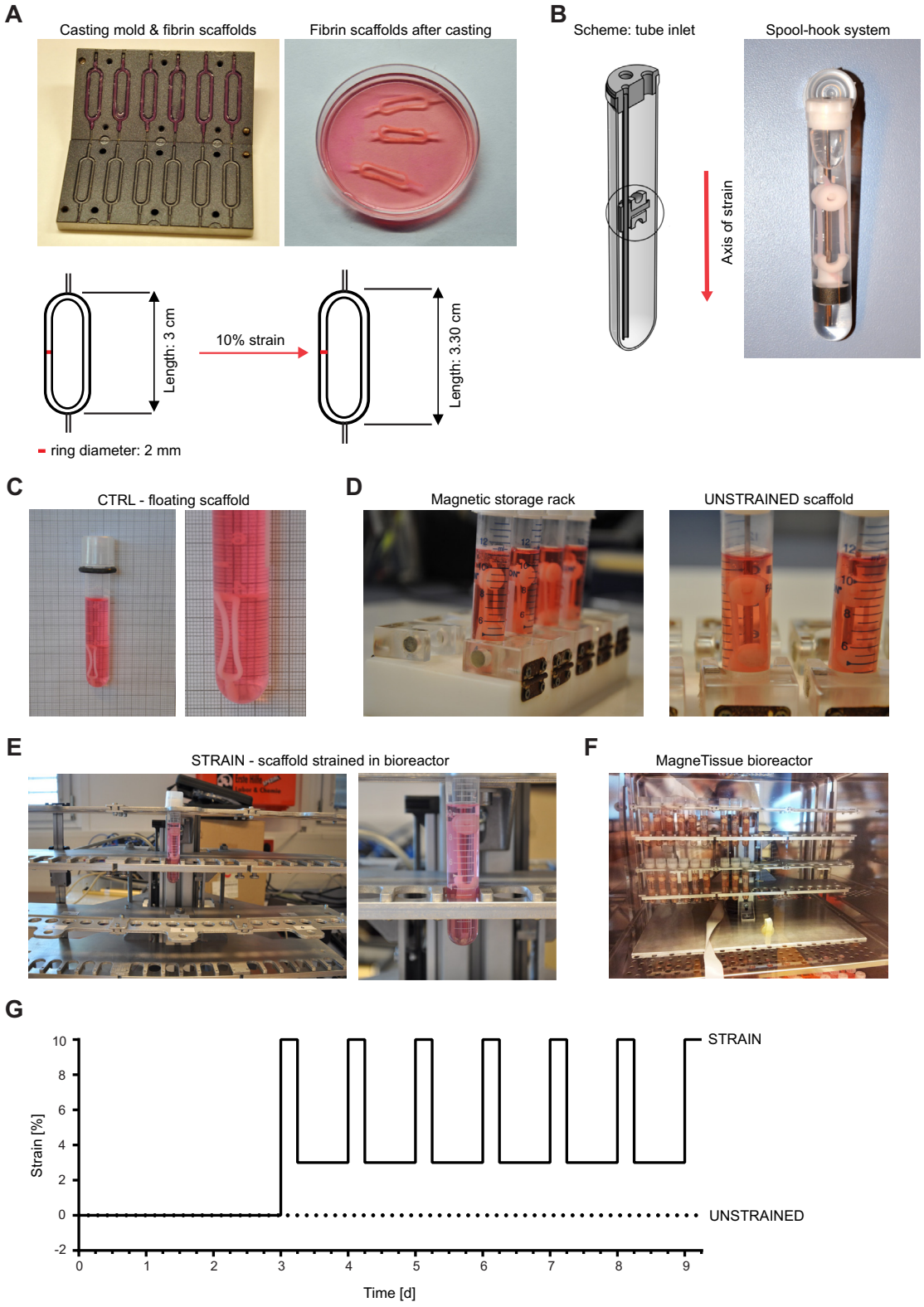

Fig. 1. The MagneTissue bioreactor system. (A) Upper left: Teflon coated mold for scaffold preparation by injection. Upper half of the mold containing six freshly cast fibrin rings. Upper right: fibrin scaffolds released from the mold after polymerization. Below: scheme displays proportions of the fibrin rings (3 cm in length and 2 mm in diameter) and the elongation during static mechanical stimulation. (B) Left: custom-made tube inlet with the spool-hook system that fibrin rings are attached to. Right: scaffold mounted onto the spool-hook system before being stored in custom-made magnetic racks at 0% strain (UNSTRAINED group) or applied to the MagneTissue bioreactor for mechanical stimulation (STRAIN group). (C) Representative image of controls (CTRL) – scaffolds embedded with C2C12 cells floating in medium. (D) Left: custom-made magnetic rack for storage of unstrained samples over the whole culture period and for the strain group before applied to the bioreactor at day 3. Right: UNSTRAINED sample stored in magnetic rack receiving 0% strain. (E) Representative image of STRAIN sample. At day 3 STRAIN samples are transferred from the magnetic rack to the bioreactor and subjected to the programmed strain protocol. (F) Custom-made MagneTissue bioreactor system, where strain is applied via magnetic force transmission and parameters are controlled via custom-made software. (G) The mechanical stimulation protocol: 3 days after construct preparation, 6 h of static strain at 10% (exercise phase) followed by 18 h at 3% (rest phase) are applied daily until the end of the culture period (day 9).

Please cite this article in press as: P. Heher et al., A novel bioreactor for the generation of highly aligned 3D skeletal muscle-like constructs through orientation of fibrin via application of static strain, Acta Biomater. (2015), http://dx.doi.org/10.1016/j.actbio.2015.06.033

incubated with the primary antibody at appropriate dilution in PBS/T-1% (w/v) BSA for 1 h at 37 °C (Desmin 1:100, MHC 1:400). After incubation with the primary antibody the samples were washed and incubated with the secondary antibody at appropriate dilution (1:400) in PBS/T-1% (w/v) BSA for 1 h at 37 °C. For nuclear visualization the samples were incubated with 4′,6-diamidi no-2-phenylindole (DAPI) diluted 1:1000 in PBS for 10 min. All immunostained samples were analyzed on a Leica SP5 confocal microscope (Leica Microsystems GmbH, Wetzlar, Germany).

2.8. Scanning electron microscopy (SEM)

Samples were fixed with 2.5% formaldehyde for 2 h at room temperature. After fixation, the fibrin rings were first cut into approximately 0.5 cm long pieces and then longitudinally for the characterization of the scaffold interior. Dehydration was performed using a graded ethanol series (40%, 50%, 60%, 70%, 80%, 90%, 100% for 15 min each) and sample incubation in a serial dilution of hexamethyldisilazane (33%, 66%, 100% in ethanol absolute, for 1 h each) was used for drying. Samples were mounted on aluminium stubs, sputter-coated with Pd–Au using a Polaron SC7620 sputter coater (Quorum Technologies Ltd., East Grinstead, United Kingdom) and examined with a JEOL JSM-6510 scanning electron microscope (JEOL GmbH, Eching/Munich, Germany).

2.9. Quantitative reverse transcription polymerase chain reaction (RT-qPCR)

At day 0, 3, 6 and 9 cells were harvested by digestion of fibrin rings in 1 mL of 100 U/mL nattokinase (Japan Bioscience Lab, California, USA) in PBS, pH 7.4 supplemented with 15 mmol/L ethylenediaminetetraacetic acid (EDTA) for 1 h at 37 °C under constant agitation, followed by total mRNA extraction using the peqGOLD total RNA Kit (VWR International GmbH, Erlangen, Germany). Per sample, 1 µg of mRNA was transcribed into cDNA with the DyNAmo cDNA Synthesis Kit (Life Technologies, Vienna, Austria). Quantitative PCR was performed with the KAPA Fast SYBR© Fast Universal Kit (VWR International GmbH, Erlangen, Germany) in a Stratagene© Mx3005P cycler (Agilent Technologies, Santa Clara, USA) in triplicates, using 10 ng of cDNA per reaction. Thermal cycle conditions were 5 min at 95 °C, followed by 40 cycles of either 10 s at 95 °C and 30 s at 60 °C (*GAPDH*, *MyoD*, *TnnT1* and *Myf5*) or 30 s at 95 °C and 1 min at 60 °C (*Myogenin*, *Desmin* and *Pax7*). Target cycle threshold (C_T) values normalized to the house keeping gene glyceraldehyde-3-phosphate dehydrogenase (GAPDH) were compared to corresponding values at each time point as well as day 0 for time dependent expression profiles using the comparative C_T ($\Delta\Delta C_T$) method. Primer sequences and primer concentrations used are listed in Table 1.

2.10. Histological analysis

All histological analyses were performed with Fiji software [42] from immunofluorescence confocal microscopy images taken at the end of the culture period (day 9). All samples were stained for MHC and nuclei were visualized with DAPI. Only MHC-positive cells containing three or more nuclei were rated as myotubes. The fusion index was calculated as the ratio of the number of nuclei in myotubes to the number of total nuclei in percent from images taken at 40× magnification. Myotube length and diameter measurements as well as myotube alignment analysis were performed with images taken at 10× magnification. Myotube alignment was calculated as the angle between the long axis of a myotube and the axis of strain/mean orientation axis (defined as 0°), with the distribution of the respective percentage of myotubes shown in 15° angle deviation intervals. The width of an individual myotube was determined as the mean of 5 measurements taken at random positions perpendicular to the long axis at the respective position. Myotube length was determined only for myotubes containing 5 or more nuclei.

2.11. Statistical analysis

All data are presented as mean + standard deviation (S.D.) except for Figs. 2A, 4G, 6B and C which are presented as box plots. For the relative expression of genes over time (Fig. 5) values are depicted as cubic spline curves. Normal distribution of data was tested with the D'Agostino & Pearson omnibus normality test. Comparisons between groups were calculated using One-way ANOVA with Tukey's multiple comparison test or Kruskal–Wallis test with Dunn's multiple comparison test and *P*-values $\leqslant 0.05$ were considered as statistically significant. All calculations were performed using GraphPad Prism Software (GraphPad Software Inc., SanDiego, USA).

3. Results

3.1. Preparation of fibrin rings and viability of 3D muscle constructs

Myogenic differentiation is highly affected by the mechanical properties of the biomaterial. Therefore, stiffness of different fibrin formulations was initially measured to find a fibrinogen concentration that yields scaffolds mimicking the stiffness of skeletal muscle which has been demonstrated to approximately range from 8 to 17 kPa [43]. Four different fibrinogen concentrations were used ranging from "soft" to "stiff" (10, 20, 30 and 40 mg/mL) and subjected to mechanical testing (Fig. 2A, left). Fibrinogen concentrations of 10 and 20 mg/mL displayed an average Young's modulus of 11.57 and 17.21 kPa, respectively, whereas higher concentrations (30 and 40 mg/mL) exceeded the modulus considered optimal for myogenesis (24.53 kPa and 31.27 kPa, respectively; Fig. 2A, middle). Although a fibrinogen concentration of 10 mg/mL seemed ideal, stiffer fibrin scaffolds (20 mg/mL fibrinogen) were used in this study, as the casting process was more reliable and the scaffolds more stable. Additionally, varying the thrombin concentration does not alter fibrin stiffness, as this is directly proportional to the fibrinogen concentration (Fig. 2A, right).

Table 1
Primer sequences and concentrations used for qPCR.

Target	Primer forward	Primer reverse	Primer conc. [nM]
GAPDH	AACTTTGGCATTGTGGAAGG	ACACATTGGGGGTAGGAACA	200
MyoD	ACTACAGTGGCGACTCAGAT	CCGCTGTAATCCATCATGCC	200
Myf5	TGACGGCATGCCTGAATGTA	GCTCGGATGGCTCTGTAGAC	200
TnnT1	AAACCCAGCCGTCCTGTG	CCTCCTCCTTTTTCCGCTGT	200
Myogenin	GGTCCCAACCCAGGAGATCAT	ACGTAAGGGAGTGCAGATTG	200
Desmin	AGAGGCTCAAGGCCAAACTAC	AGGGATTCGATTCTGCGCTC	200
Pax7	CGTAAGCAGGCAGGAGCTAA	ACTGTGCTGCCTCCATCTTG	400

Please cite this article in press as: P. Heher et al., A novel bioreactor for the generation of highly aligned 3D skeletal muscle-like constructs through orientation of fibrin via application of static strain, Acta Biomater. (2015), http://dx.doi.org/10.1016/j.actbio.2015.06.033

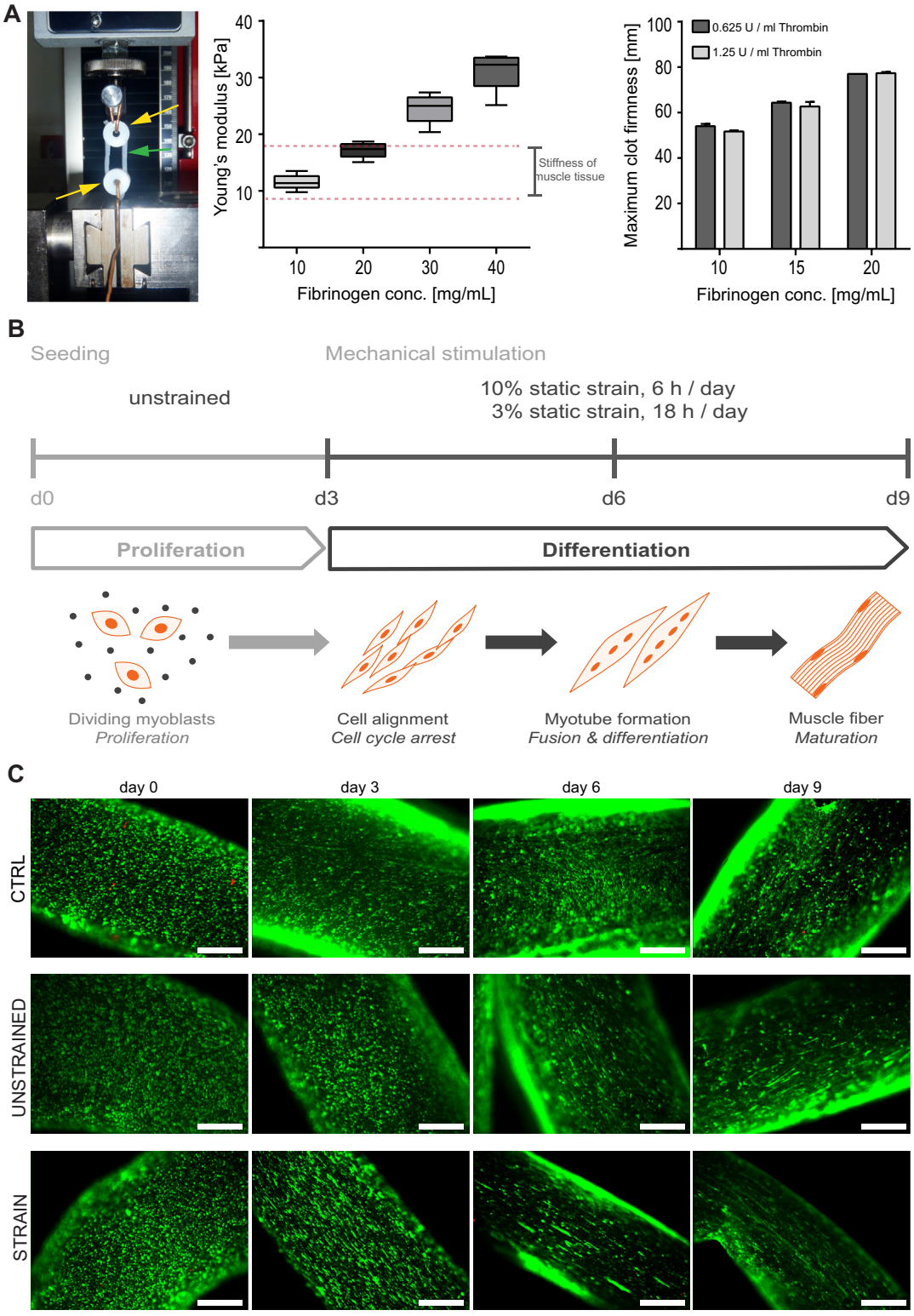

Fig. 2. Scaffolds mimic the mechanical properties of native skeletal muscle and viability is not impaired in 3D cell-scaffold constructs. (A) Left: mechanical test setup for fibrin scaffolds. Fibrin rings are mounted onto the same spools as used in the bioreactor. Yellow arrows – spools; green arrow – fibrin ring. Middle: box plots depict the Young's modulus of scaffolds with increasing fibrinogen concentrations as indicated ($n = 5$). The Young's modulus within the red dashed lines marks the range of the stiffness of skeletal muscle as proposed in [47]. Right: maximum clot firmness of fibrinogen and thrombin concentrations as indicated ($n = 3$; mean + S.D. (error bars)). (B) Schematic representation of experimental design and working hypothesis. At day 0 ring-shaped fibrin scaffolds with embedded cells were cast and either assigned controls (floating in medium), unstrained samples (assembled on spool-hook system and kept at 0% strain) or strain samples (assembled on spool-hook system receiving static strain). The first two days, cells in scaffolds were allowed to recover from encapsulation and to proliferate. At day 3, the first round of 10% static strain for 6 h was applied to the strain group followed by a rest phase of 18 h at 3% strain. This stimulation protocol was repeated daily until inclusively day 9. During the culture period the cells started to align and withdrew from the cell cycle, followed by fusion and differentiation into myotubes. (C) Calcein AM (green)/PI (red) staining was performed at day 0, 3, 6 and 9 in controls, unstrained and strained rings to assess viability and morphological changes over time. Scale bars represent 500 μm. CTRL = control, UNSTRAINED = unstrained rings, STRAIN = strained rings. (For interpretation of the references to color in this figure legend, the reader is referred to the web version of this article.)

Please cite this article in press as: P. Heher et al., A novel bioreactor for the generation of highly aligned 3D skeletal muscle-like constructs through orientation of fibrin via application of static strain, Acta Biomater. (2015), http://dx.doi.org/10.1016/j.actbio.2015.06.033

For the generation of 3D skeletal muscle constructs, we prepared ring-shaped fibrin scaffolds in which cells were homogenously distributed (representing day 0). For the following 2 days the scaffolds with embedded cells were either kept floating in media (control group, Fig. 1C) or assembled onto the spool-hook system and stored in a magnetic rack – representing the unstrained control group (Fig. 1D) and the strained group (Fig. 1E). This initial period was chosen as to allow cell adaption to their new environment and propagate further proliferation, as cell density is a crucial factor for proper myoblast fusion and differentiation [19]. At day 3 differentiation was initiated and a daily static mechanical stimulation protocol consisting of 6 h at 10% strain followed by 18 h at 3% strain was performed for the strain group (Fig. 1E and G) until the end of the culture period (Fig. 2B). The rationale behind this protocol was to induce cell alignment in order to facilitate directed myotube formation in combination with a physiological mechanical stimulus to promote myogenic differentiation and maturation.

We assessed viability of the cells embedded in the fibrin rings by Calcein AM and PI staining (Fig. 2C). Over the culture period of 9 days viability was not impaired in any experimental group. Additionally, the macroscopic appearance of cells in the strained constructs at day 3 demonstrated a higher degree of alignment already after the first cycle of static stimulation, whereas in the control and unstrained group no such phenomena were observed. Alignment was even more prominent at day 6 and 9 in the strain group, compared to partial alignment of the cells in the unstrained and random orientation in the control group (Fig. 2C). Putative myotube formation could be observed from day 6 on in the strain group highlighted by the presence of elongated structures of Calcein AM-positive cells (Fig. 2C, lower panel). These data demonstrate that our experimental setup as well as the chosen composition of the biomaterial and the extent of static strain were appropriate as viability was not impaired and first morphological changes due to mechanical stimulation were observed.

3.2. Static strain induces fibrin fibril alignment and cellular orientation

To gain deeper insight into the effects of static mechanical stimulation in our system and how it affects fibrin and the incorporated cells, SEM analysis was performed at different time points. First, we analyzed the effect of a single round of stimulation of 6 h at 10% strain. Fibrin fibrils of control and unstrained samples displayed random orientation whereas in strained samples fibril alignment along the axis of strain was highly increased (Fig. 3A, left). As expected, application of strain resulted in thorough cellular alignment compared to control samples where this effect was not observed. Unstrained samples, however, displayed altered cellular morphology compared to the controls, with partially aligned cells as a result of scaffold anchoring (Fig. 3A, right). On day 9, scaffold microstructure was similar to day 3, with random fibril orientation in the control and unstrained groups and preserved alignment in the strain group (Fig. 3B, left). In contrast to control samples, both unstrained and strained samples showed a higher degree of cellular alignment (Fig. 3B, right). Repeated cycles of static strain resulted in preservation of fibril alignment, as the interior and the surface of strained fibrin rings displayed overall uniaxial fibril and cell alignment at the end of the culture period. Scaffold anchoring (unstrained group) did not elicit changes in fibrin microstructure, nevertheless it promoted cellular alignment over time. In order to characterize if the observed strain-induced effect on the biomaterial was directly translated to the cells we performed immunofluorescence staining for the structural muscle marker Desmin [44,45]. As expected, no noticeable changes in alignment were present in floating control samples, whereas unstrained samples displayed aligned cells to some extent. In contrast, one cycle of stimulation already had a thorough effect on the morphology and alignment of the cells. Static strain at 10% for 6 h resulted in pronounced cell alignment, with elongated cells oriented in the direction of strain. Moreover, this effect was accompanied by the transition of nuclear morphology from a round to a stretched shape, a strong indicator for cellular polarity [46] (Fig. 3C).

3.3. Repetitive static mechanical stimulation promotes myotube formation in a highly oriented manner

In order to substantiate the hypothesis that our repetitively applied static strain protocol enhances myogenic differentiation, myotube formation and alignment were analyzed after 6 days of stimulation. In general, mouse myoblasts differentiated on tissue culture dishes readily form multi-nucleated myotubes, however, with a high degree of myotube branching and random orientation (Fig. 4A). Myotube branching was not observed when myoblasts were differentiated on top of a fibrin substratum (20 mg/mL fibrinogen and 0.625 U/mL thrombin) for 6 days. In addition, a higher degree of sarcomeric patterning was evident compared to the 2D tissue culture plastic control (Fig. 4B). This effect is linked to the matrix properties as striations have been shown to primarily develop on substrates with a stiffness comparable to native muscle [47]. Looking at the situation in 3D, we observed that in all three experimental conditions myoblasts differentiated to MHC-positive myotubes until day 9. However, similar to the results obtained from the 2D differentiation experiments (Fig. 4A and B), myotubes from the control group were randomly oriented. In comparison, the unstrained samples exhibited a higher degree of myotube alignment with an increased fraction of elongated nuclei. The strain group demonstrated that the applied static mechanical stimulation protocol led to the formation of highly aligned myotubes which appeared to be thicker compared to their control counterparts (Fig. 4C). Notably, sarcomeric patterning of myotubes in the strain group was more pronounced, indicating a higher degree of maturity (see also Fig. 6). To further characterize the qualitatively observed morphological findings the overall myotube alignment was quantified (Fig. 4D). More than 85% of all analyzed myotubes in the strain group were aligned in the direction of strain and the residual 15% showed a 15–30° deviation from the axis of strain. Approximately 70% of all myotubes analyzed in the unstrained group did not deviate more than 15° from the axis of strain, about 25% were 15–30° off and a very small percentage was 30–45° off. In comparison to these two groups the myotubes of the control group displayed deviations from the axis of strain/mean orientation axis at all angles, confirming random orientation (Fig. 4D).

Macroscopically, application of static mechanical strain for 6 days led to the generation of a construct consisting of a densely packed array of parallel myotubes reaching lengths of approximately 1 mm (Fig. 4E), which mirrors essential characteristics of native muscle tissue (Fig. 4F). In order to quantify the efficiency of myotube formation the fusion index was determined at the end of the culture period. The application of strain led to a significant increase in myocyte fusion compared to the control as well as to the unstrained group. The fusion index of controls was 15%, 20% in the unstrained group and reached 30% in the strain group, which roughly corresponds to a 2-fold and a 1.7-fold increase in myocyte fusion compared to the control and to the unstrained control, respectively (Fig. 4G).

3.4. Static strain significantly enhances expression of myogenic markers and highly improves muscle differentiation

With the notion that static strain appeared to strongly augment myogenic differentiation morphologically, we also tracked

Please cite this article in press as: P. Heher et al., A novel bioreactor for the generation of highly aligned 3D skeletal muscle-like constructs through orientation of fibrin via application of static strain, Acta Biomater. (2015), http://dx.doi.org/10.1016/j.actbio.2015.06.033

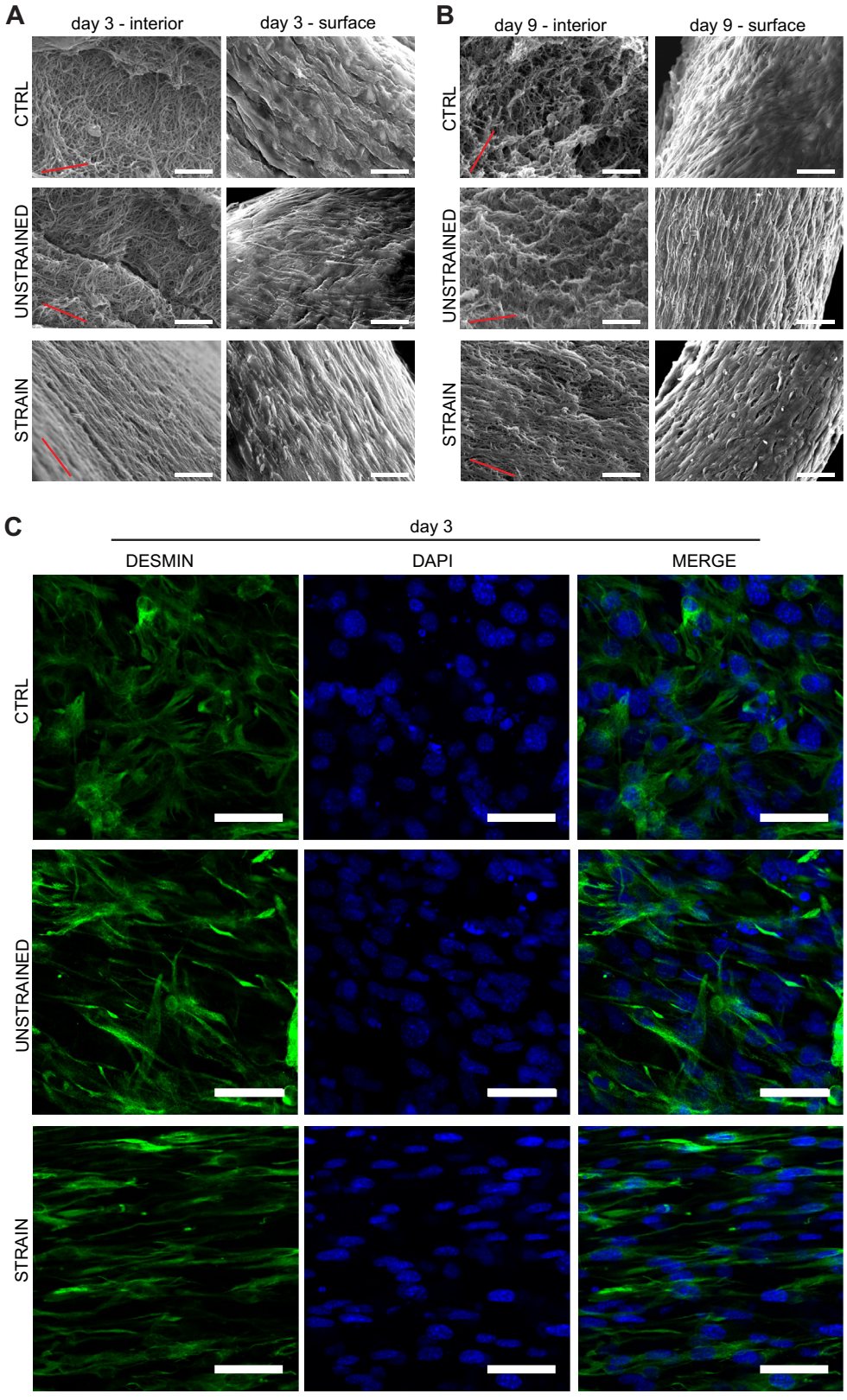

Fig. 3. Mechanical strain leads to uniaxial fibrin fibril alignment and affects cell orientation. (A) To visualize changes in fibril alignment of the scaffolds after one round of mechanical stimulation (10% for 6 h) at day 3, control, unstrained and strained samples were fixed and subjected to SEM analysis. Representative images of the interior (left) and surface (right) of the scaffolds are shown. Red bars indicate mean orientation axis. (B) Control, unstrained and strained rings were fixed after the last round of mechanical stimulation at day 9 and SEM imaging was performed. Representative images of the interior (left) and surface (right) of the scaffolds are shown. Red bars indicate mean orientation axis. (C) Control, unstrained and strained fibrin rings after one round of 10% static strain for 6 h at day 3. Scaffolds were fixed after mechanical stimulation was completed (STRAIN) along with the controls and the unstrained samples and subsequently stained for Desmin (green, left). A nuclear counterstain with DAPI (blue, middle) was performed. Scale bars represent 5 μm (A, B left panel) and 50 μm (A, B right panel; C), respectively. CTRL = control, UNSTRAINED = unstrained rings, STRAIN = strained rings. (For interpretation of the references to color in this figure legend, the reader is referred to the web version of this article.)

Please cite this article in press as: P. Heher et al., A novel bioreactor for the generation of highly aligned 3D skeletal muscle-like constructs through orientation of fibrin via application of static strain, Acta Biomater. (2015), http://dx.doi.org/10.1016/j.actbio.2015.06.033

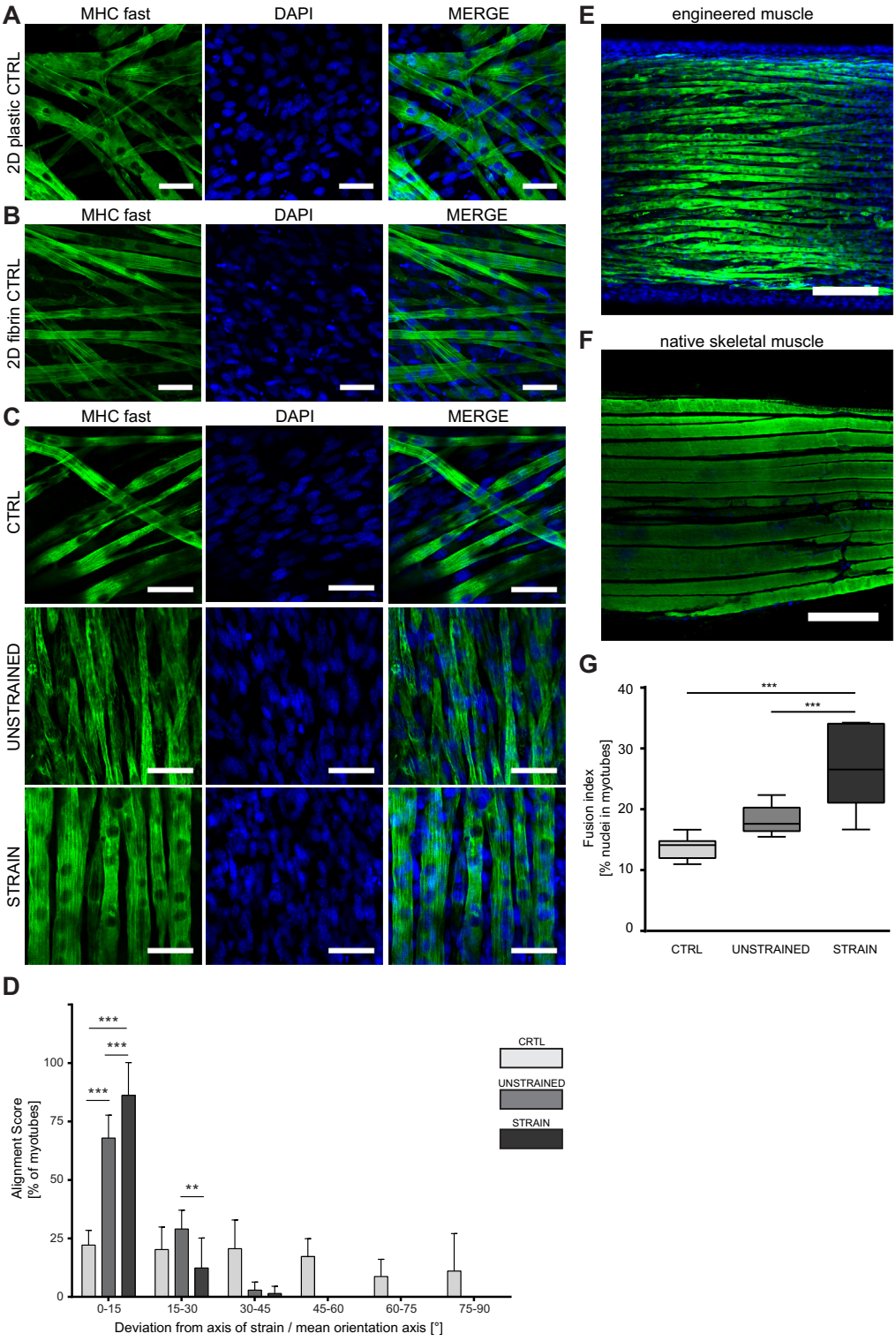

Fig. 4. Application of strain promotes alignment of myotubes and augments myocyte fusion as well as muscle differentiation on the morphological level. (A) Cells grown on cell culture plastic serving as 2D controls were differentiated for 6 days and then stained for MHC fast (green, left) and a nuclear counterstain with DAPI (blue, middle) was performed. (B) Cells were grown on top of a fibrin matrix with the same composition as in the 3D constructs and differentiated for 6 days. Myotubes were then stained for MHC fast (green, left) and a nuclear counterstain with DAPI (blue, middle) was performed. (C) Control, unstrained and strained fibrin rings after 7 rounds of static mechanical stimulation and 6 days of differentiation were fixed at day 9. Whole rings were stained for MHC fast (green, left) and a nuclear counterstain with DAPI (blue, middle) was performed. (D) Alignment score giving the deviation of the long myotube axis from the axis of strain/mean orientation axis at day 9 calculated for control, unstrained and strained fibrin rings. Values are given in % ($n = 9$ of three independent experiments; mean + S.D. (error bars); $^{**}p < 0.01$; $^{***}p < 0.001$; one-way ANOVA with Tukey's multiple comparison test). (E) Strained fibrin rings at day 9 were stained for MHC fast (green) and DAPI for nuclear counterstain (blue). Overlay image is shown. (F) Longitudinal section of a native mouse skeletal muscle (adductor femoris) stained for MHC fast (green) and DAPI for nuclear counterstain (blue). Overlay image is shown. (G) The fusion index, representing the percentage of nuclei within myotubes relative to total nuclei, was analyzed at day 9 for all three experimental groups ($n \geqslant 7$ of three independent experiments with more than 1000 nuclei analyzed per group; $^{***}p < 0.001$; one-way ANOVA with Tukey's multiple comparison test). Scale bars represent 50 μm (A–C) and 250 μm (E and F), respectively. CTRL = control, UNSTRAINED = unstrained rings, STRAIN = strained rings. (For interpretation of the references to color in this figure legend, the reader is referred to the web version of this article.)

Please cite this article in press as: P. Heher et al., A novel bioreactor for the generation of highly aligned 3D skeletal muscle-like constructs through orientation of fibrin via application of static strain, Acta Biomater. (2015), http://dx.doi.org/10.1016/j.actbio.2015.06.033

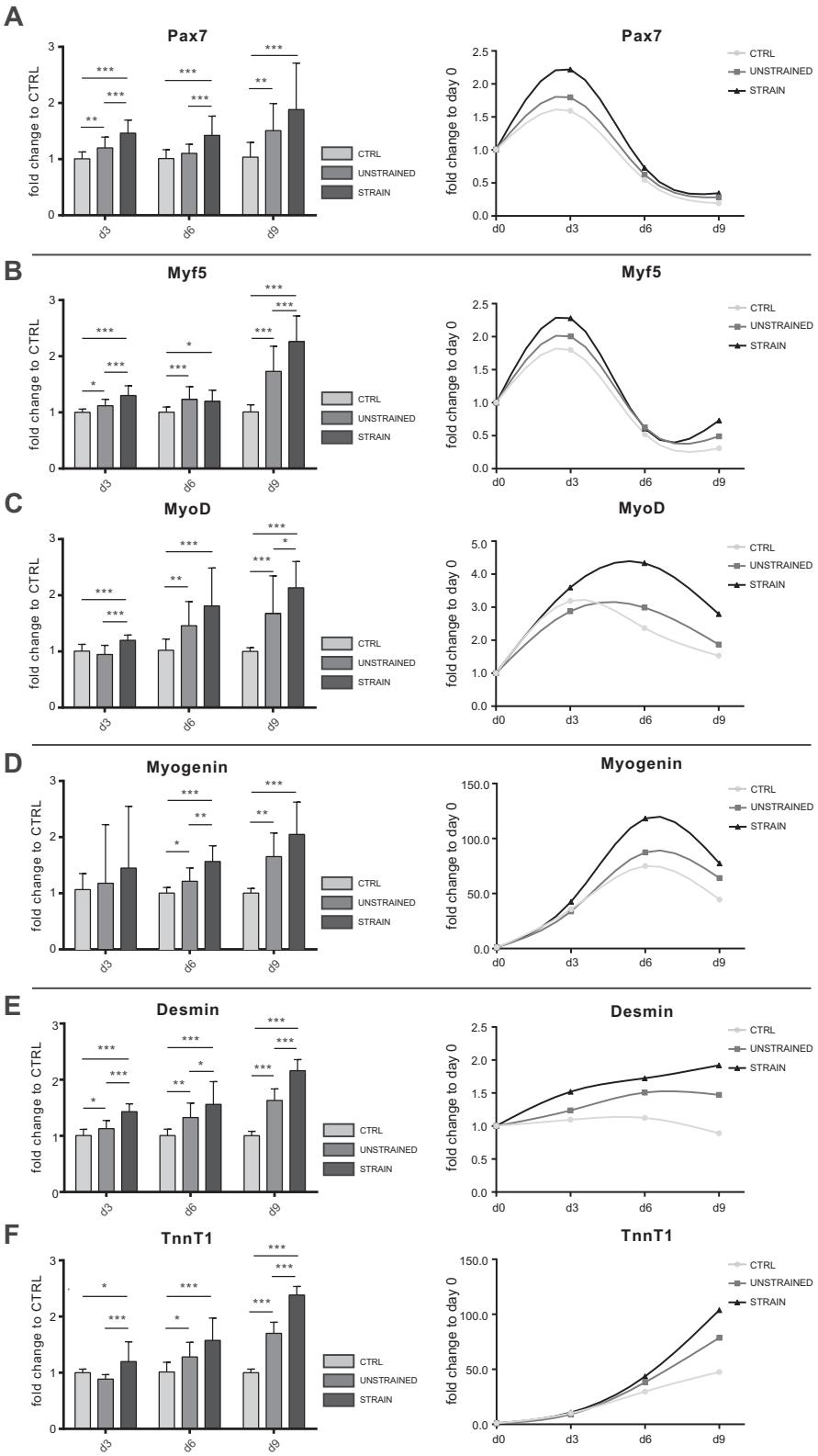

Fig. 5. Mechanical strain enhances expression of early, mid and late stage-specific myogenic markers. Total mRNA was isolated and RT-qPCR for a set of myogenic marker genes was performed. Bar graphs (left) depict fold change of expression levels normalized to controls at the indicated timepoints. Cubic spline curves (right) show relative expression over time, with fold induction normalized to day 0 within each group ($n = 6$ in triplicates of two independent experiments; mean + S.D. (error bars); $^{*}p < 0.05$; $^{**}p < 0.01$; $^{***}p < 0.001$) (A) *Pax7* expression levels. One-way ANOVA with Tukey's multiple comparison test (day 3 and day 6) or Kruskal–Wallis test with Dunn's multiple comparison test (day 9). (B) *Myf5* expression levels. One-way ANOVA with Tukey's multiple comparison test (day 3 and day 9) or Kruskal–Wallis test with Dunn's multiple comparison test (day 6). (C) *MyoD* expression levels. One-way ANOVA with Tukey's Multiple comparison test (day 3 and day 9) or Kruskal–Wallis test with Dunn's multiple comparison test (day 6). (D) *Myogenin* expression levels. Kruskal–Wallis test with Dunn's multiple comparison test. (E) *Desmin* expression levels. One-way ANOVA with Tukey's multiple comparison test (F) *TnnT1 expression levels.* One-way ANOVA with Tukey's multiple comparison test (day 3 and day 9) or Kruskal–Wallis test with Dunn's multiple comparison test (day 6). TnnT1 = Troponin T1; CTRL (light gray) = control, UNSTRAINED (middle gray) = unstrained rings, STRAIN (dark gray) = strained rings.

Please cite this article in press as: P. Heher et al., A novel bioreactor for the generation of highly aligned 3D skeletal muscle-like constructs through orientation of fibrin via application of static strain, Acta Biomater. (2015), http://dx.doi.org/10.1016/j.actbio.2015.06.033

transcriptional levels of muscle specific marker genes over time with RT-qPCR to elucidate the performance of the bioreactor system in a more thorough manner. We chose to analyze a combination of early (*Pax7, Myf5, MyoD*), mid (*Myogenin*) and late stage-specific/structural (*TnnT1, Desmin*) myogenic markers to observe the effects of static strain in the cascade of myogenic specification, differentiation and maturation.

Paired box homeodomain gene *Pax7* is an upstream transcriptional regulator of all four myogenic regulatory factors (MRFs) and essential for the activation of satellite cells and their commitment to the myogenic lineage by induction of *MyoD* [48,49]. *Pax7* has been shown to be highly expressed in activated satellite cells as well as, at low levels, proliferating myoblasts and is downregulated as the cells differentiate [50,51]. After the onset of differentiation (day 3), this downregulation was observed in all three treatment groups (Fig. 5A, right graph). Surprisingly, compared to the control, *Pax7* expression was slightly upregulated in the unstrained and, to a higher extent, in the strain group which received one cycle of static strain for 6 h at 10% at day 3 before induction of differentiation (Fig. 5A, left graph). Although *Pax7* expression was expectedly downregulated during differentiation the strain group seemed to keep elevated *Pax7* levels compared to the control groups until day 9 (Fig. 5A, left graph). *Myf5*, *MyoD*, and *Myogenin* are basic helix loop helix transcription factors that belong to the MRFs [52], with *Myf5* and *MyoD* required for myoblast determination and *Myogenin* essential for terminal differentiation into myotubes [53]. The three MRFs peak in a temporal manner, with *Myf5*, although moderately expressed, being the first at day 3 (Fig. 5B, right graph) followed by both *MyoD* (Fig. 5C, right graph) and *Myogenin* (Fig. 5D, right graph) that peak at day 6. In comparison to the control and the unstrained group, application of static strain resulted in slightly higher expression of *Myf5* (Fig. 5B, left graph). *MyoD* on the other hand was influenced later than *Myf5* (Fig. 5C, right graph). By day 6, a gradual significant increase in *MyoD* expression could be observed in the unstrained (~1.5-fold) and the strain group, with the strain group displaying an approximately 1.8–2-fold induction compared to the control (Fig. 5C, left graph). This effect might be directly linked to the observed upregulation of both *Pax7* and *Myf5* – two transcription factors acting upstream of *MyoD* – at the onset of differentiation [54]. *Myogenin* expression has been shown to be upregulated after the induction of *Myf5* and *MyoD* [55] and did not differ on day 3 between the different experimental groups. However, after 3 days of differentiation (day 6) *Myogenin* expression was almost 1.6-fold increased in the strain group compared to the control group and 1.4-fold increased compared to the unstrained group. At day 9 the expression of the unstrained group and the strain group compared to the control remained elevated 1.7-fold and 2-fold, respectively (Fig. 5D, left graph), even though *Myogenin* expression in general peaked after 3 to 4 days of differentiation (Fig. 5D, right graph).

A very important aspect of skeletal muscle tissue engineering is the development of functional muscular ultrastructure. Thus, we analyzed the expression of two different structural marker genes, *Desmin* and *Troponin T1* (*TnnT1*). Desmin, a muscle-specific intermediate filament, is one of the earliest structural genes expressed in myogenesis and already expressed in satellite cells and proliferating myoblasts [44]. Desmin filaments encircle the Z-disk, holding the actin filaments together and hence play a fundamental role in transmitting tension throughout the myofibril [45]. *Desmin* was significantly higher expressed in the strain group (at day 6 1.5-fold and more than 2-fold at day 9) compared to unstrained samples and controls (at day 6 1.3-fold and more than 1.5-fold on day 9; Fig. 5E, left graph). Overall, *Desmin* expression levels remained rather constant over time, with a moderate induction in the unstrained group and a more thorough induction when static strain was applied (Fig. 5E, right graph). TnnT1 is the tropomyosin binding subunit of the troponin complex and as such plays an important role in Ca^{2+}-induced striated muscle contraction [56,57]. Analysis of *TnnT1* therefore delivers an important read-out for the functionality and maturity of skeletal muscle tissue [57]. On day 9, *TnnT1* expression was significantly enhanced in the strain group compared to the control (2.5-fold increase), while the unstrained group displayed an increase of almost 1.75-fold compared to the control (Fig. 5F, left graph). Over the culture period of 9 days, *TnnT1* relative expression levels increased in all three experimental groups (Fig. 5F, right graph).

In accordance with the results of the morphological analysis the qPCR data demonstrated that: (i) myogenesis was not impeded in the 3D fibrin-cell scaffolds, as myotube formation could readily be observed in the controls and myogenic expression patterns progressed normally, with temporal regulation; (ii) unstrained scaffolds (resembling anchored scaffolds) displayed a better performance morphologically as well as on the gene expression level compared to controls, due to contractile force generation in combination with scaffold polarity [10,34,58]; (iii) with the application of static strain (10%) for 6 h daily followed by a rest phase (3%) for 18 h this effect could be markedly enhanced and led to significantly better alignment and higher expression levels of an essential set of myogenic markers in regard to induction of differentiation and myotube formation.

3.5. Application of static strain enhances muscle maturity

After we demonstrated an improvement in alignment and enhanced differentiation on the morphological and molecular level when strain was applied, we wanted to find out whether this induction was also linked to enhanced myotube maturity. Immunostaining for MHC and subsequent qualitative morphological analysis revealed a much higher occurrence of sarcomeric patterning in myotubes of the strain group (Fig. 6A), a structural feature directly linked to contractile force, indicating a higher degree of maturity. As myotubes appeared to be thicker when strain was applied (Fig. 4C, lower panel), myotube length and diameter were determined. In accordance with previously published studies [27,59], unstrained constructs displayed enhanced myotube length and diameter compared to controls. However, this effect was further increased when strain was applied, as myotubes in the strain group were significantly thicker (~20%) and longer (~30%) than in unstrained samples, with myotubes reaching a maximum length of 1 mm (Fig. 6B and C).

Altogether, these findings strongly support the hypothesis that static mechanical stimulation positively affects *in vitro* myogenesis on several levels: a higher degree of alignment promotes parallel myotube formation accompanied by enhanced gene expression levels of early, mid and late stage-specific marker genes which ultimately yields muscle constructs with a highly aligned array of myotubes displaying increased maturity.

4. Discussion

Despite recent advances in the field of musculoskeletal tissue engineering, the *in vitro* generation of skeletal muscle constructs with structural and functional characteristics comparable to those *in vivo* is still a major challenge to overcome. Thus, scientists still seek feasible strategies to obtain mature, long, functional muscle fibers in volumetric constructs, with proper vascularization and innervation of the tissue. Proposed approaches to engineer muscle (-like) tissue range from scaffold anchoring [10,40,58] or micropatterning of biomaterials for guided myotube formation [39,60,61] to electrical [36–39,62] or mechanical stimulation in bioreactors in

Please cite this article in press as: P. Heher et al., A novel bioreactor for the generation of highly aligned 3D skeletal muscle-like constructs through orientation of fibrin via application of static strain, Acta Biomater. (2015), http://dx.doi.org/10.1016/j.actbio.2015.06.033

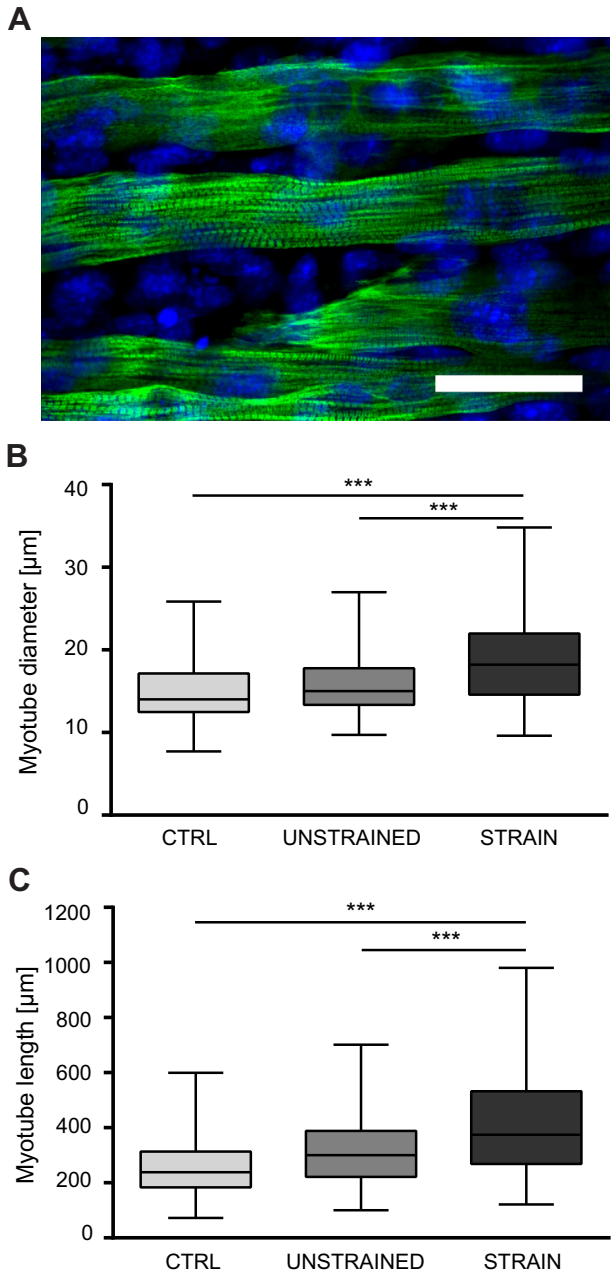

Fig. 6. Static strain improves sarcomeric patterning and increases myotube length and diameter – three indicators for muscle maturity. (A) Representative immunofluorescence image of a strained sample at day 9 stained for MHC fast (green) and DAPI for nuclear counterstain (blue). Overlay image is shown. Scale bar represents 50 µm. (B) Quantification of myotube diameter at day 9 ($n \geqslant 8$ of three independent experiments with at least 146 myotubes per group analyzed; $^{***}p < 0.001$; Kruskal–Wallis test with Dunn's multiple comparison test). (C) Quantification of myotube length at day 9 ($n \geqslant 7$ of three independent experiments with at least 202 myotubes per group analyzed; $^{***}p < 0.001$; Kruskal–Wallis test with Dunn's multiple comparison test). CTRL = control, UNSTRAINED = unstrained rings, STRAIN = strained rings. (For interpretation of the references to colour in this figure legend, the reader is referred to the web version of this article.)

2D [29,31,63–65] and 3D settings [6,9,11,14,27,66–68]. However, while there is a clear consensus in the field concerning the necessity for mechanical stimulation in 3D skeletal muscle tissue engineering, not all available systems offer programmable and individually adjustable control over strain parameters. Thus, software-controlled systems capable of applying tunable strain regimes (ramp, cyclic and static) are emerging as a very promising approach [9,27,41,69,70].

With regard to the current limitations in skeletal muscle tissue engineering [67], we have established a custom-made closed bioreactor system (MagneTissue) which applies mechanical strain in a cyclic, static or ramp manner to cells embedded in a fibrin matrix via magnetic force transmission. Our results indicate that application of 10% static strain for 6 h followed by a rest phase at 3% led to vastly improved alignment of both the biomaterial and the cells. As a consequence, myoblasts fused along the axis of strain in a highly ordered manner, resulting in a parallel array of myotubes with increased size and more pronounced sarcomeric patterning compared to controls. Additionally, our qPCR data verified static mechanical stimulation as an essential and potent regulator of early myogenesis, as structural genes important for muscle function and contractility were significantly upregulated when strain was applied, emphasizing the importance of mechanotransduction in muscle tissue engineering [26].

Choosing a biomaterial whose mechanical properties mimic those of skeletal muscle tissue is crucial for myogenic differentiation. Fibrin hydrogels are, to some extent, tunable in regard to stiffness, pore size, degradability and fibril diameter [15,16,58,71,72]. In contrast to other approaches using rather low fibrinogen to thrombin ratios [10,11,34,39], we chose a higher ratio (20 mg/mL fibrinogen, 0.625 U/mL thrombin) in our experimental setup for several reasons: (i) the stiffness is directly proportional to the fibrinogen concentration. The obtained constructs displayed a Young's modulus of about 17 kPa, which lies within the stiffness range proposed to be most suitable for myogenic differentiation [43,47,73]; (ii) the fibrinogen to thrombin ratio directly correlates with permeability and pore size as well as the ultimate tensile strength of the scaffold [16]; (iii) lower thrombin concentrations give slower clotting times, increasing the homogeneity of the fibrin meshwork, and have less detrimental effects on cell viability [74].

After testing different mechanical stimulation protocols in preliminary experiments we found that a static strain period of 10% for 6 h followed by 18 h at 3% gave optimal results in terms of cell alignment, myoblast fusion, myogenic differentiation and myotube maturity. The rationale behind this stimulation protocol is to mimic *in vivo* muscle development during embryogenesis. Due to its attachment to bone, nascent muscle is subjected to strain as a consequence of bone growth, which is supposed to facilitate myofiber alignment and augment muscle maturation. This strain was calculated to be approximately 2–3% [6,75], therefore we used a stimulation of 3% as baseline strain for the constructs. Additionally, we added a daily strain period of 10% for 6 h to provide a simulated isometric exercise stimulus. 6 h of static stimulation have been demonstrated to lead to a thorough induction of signaling pathways related to myogenic differentiation (ERK, p38MAPK, AKT) on one hand and to the activation of a subset of key myogenic differentiation markers like *Myocyte Enhancer Factor 2C (MEF2C)*, *Myogenin* or *MHC* on the other [63]. These data support our mechanical stimulation parameters of 3% and 10% alternating static strain per day as we could also show an improved myogenic outcome demonstrated by enhanced myogenic marker induction in response to strain (Figs. 4 and 5). A difference to other recently published approaches is that we do not apply cyclic strain to the constructs. The application of cyclic stimulation might also be a potent stimulus, however, previous reports indicate rather contradictory outcomes ranging from improved myogenic differentiation to enhanced proliferation and impaired muscle formation [29–32,68]. In preliminary studies we tested different mechanical stimulation protocols such as 1 h of cyclic or static strain. We found that the primary response of the cells to cyclic stimulation was a delayed onset of myogenic differentiation (data not shown). On the contrary, 1 h of static strain daily from day 3 on improved myogenesis but not to the same extent as with our current stimulation protocol. A combination of first cyclic then static strain (data

Please cite this article in press as: P. Heher et al., A novel bioreactor for the generation of highly aligned 3D skeletal muscle-like constructs through orientation of fibrin via application of static strain, Acta Biomater. (2015), http://dx.doi.org/10.1016/j.actbio.2015.06.033

not shown) could also not compete with the myogenic outcome achieved with 6 h 10% static strain and 3% strain at rest phase. Thus, we hypothesize that, in early stages of muscle differentiation, uniaxial static strain is superior to cyclic strain as it more closely recapitulates the native situation in muscle development and growth [6,75]. Nevertheless, there is substantial evidence that cyclic strain might act as an upregulatory stimulus for muscle hypertrophy and maturation at later stages of myogenesis, when myotubes have already formed [27].

Our gene expression data demonstrates that myogenesis within the constructs follows a temporal sequence in accordance with the proposed induction pattern of myogenic markers during differentiation [76]. However, we obtained interesting results regarding the expression of *Pax7*. C2C12 cells are a rhabdomyosarcoma-derived myoblast line and only weakly express *Pax7* [77]. Even though the precise role of *Pax7* is still under debate, induction of *Pax7* expression is largely considered a unique property of quiescent satellite cells re-entering the cell cycle [78]. This process is stimulated by injury or exercise such as strain *in vivo*, as well as by culture in mitogen rich media *in vitro* [79]. It is known that satellite cells undergo rapid proliferation concomitant with an upregulation of *Pax7* before initiation of differentiation (accompanied by upregulation of myogenin) [80]. Assuming that C2C12 myoblasts behave similar to satellite cells it can be speculated that culture of the cells embedded in fibrin could have a beneficial effect on proliferation compared to cell culture plastic. This might account for the global increase of *Pax7* expression between day 0 and day 3 of culture in all treatment groups. The increase in *MyoD* expression that is observed between day 0 and day 3 in all groups supports this theory, as proliferating satellite cells are characterized by co-expression of *MyoD* and *Pax7* [81]. Additionally, it has been demonstrated that, even in immortalized cell lines such as C2C12, not all cells undergo myogenic differentiation as a subset remains in quiescence [82]. This could explain the continuously elevated expression levels in the strain and unstrained groups, as the application of strain and/or endogenously generated cell-mediated strain could potentially cause partial activation of this quiescent sub-population. Considering the increased expression of *Pax7* after application of strain, it is not surprising that downstream targets *Myf5* and *MyoD*, who in turn regulate *Myogenin* expression, follow the same pattern of treatment group-specific increase in expression levels. However, in terms of expression of structural genes such as *TnnT1*, a marker for muscle contractility, another potential regulatory mechanism might be strain-induced opening of Ca^{2+} channels. It has previously been reported that mechanical stimulation increases intracellular Ca^{2+} concentrations in human lung fibroblasts [83], human pulmonary microvascular endothelial cells [84] and neonatal rat myocytes [85] in a transient manner. The transient increase in intracellular Ca^{2+} levels shows a similar pattern as observed by Takayama et al. after electrical stimulation of C2C12-derived myotubes. Their study demonstrated that responsiveness to electrical stimulation was greater in myotubes displaying a higher degree of alignment and fusion, ultimately leading to an increase in myotube contractility [86]. Connecting the higher responsiveness to intracellular Ca^{2+} levels when myotube alignment and fusion are increased to an increase in myotube contractility offers a feasible explanation for the strain-dependent upregulation of *TnnT1* expression in the strain and unstrained groups. This theory is additionally supported by the fact that, compared to day 3, the difference in *TnnT1* expression levels between the treatment groups is increased at day 6 and 9, when myotubes have already formed.

Overall, we found that static mechanical stimulation elicited a more thorough induction of the myogenic program, as the activation of myogenic determination factors at early stages of the culture protocol seems to propagate downstream, ultimately resulting in higher induction of structural and contractile marker gene expression.

Muscle tissue *in vivo* is naturally exposed to mechanical strain as a consequence of movement and exercise. This inherent susceptibility of muscle to mechanical stimulation has been exploited in many skeletal muscle tissue engineering approaches using strain not just to generate alignment but also as a way to improve myogenic differentiation and maturation [9,11,27,67,75,87]. Thus, elucidating optimized patterns potentially consisting of both static and cyclic strain will be an important step to improve the performance of skeletal muscle engineering strategies. Besides, automated systems allowing for adjustable strain regimes will be valuable to study the role of mechanotransduction in myogenesis. In this respect, the MagneTissue bioreactor system offers a feasible platform to engineer skeletal muscle-like tissue as it utilizes mechanical stimulation of otherwise free-standing constructs to generate a combination of cell alignment and a myogenic differentiation stimulus that can be voluntarily controlled. Even the quite simple static stimulation protocol we used resulted in significantly improved myogenic differentiation on the morphological and molecular level compared to anchored constructs. As expected, scaffold anchoring (represented by the unstrained group in our setup) augmented the myogenic outcome but, nevertheless, better results were obtained when strain was applied. Additionally, strained constructs displayed longer myotubes, which has already been shown in one of the earliest myogenesis models established by Vandenburgh et al. in 1983, where a passive strain of 10–12% applied to avian skeletal myotubes was used [59]. In another study by this group, human bioartifical muscles were stimulated with the use of a mechanical cell stimulator applying static and, subsequently, cyclic ramp strain, which resulted in a 12% (from 6.4 to 7.1 μm) increase in myofiber diameter [27]. With the use of the MagneTissue bioreactor system in a murine myogenic setting, myotube diameter was increased by roughly 20% from 15.7 μm in the unstrained group to almost 18.8 μm, reaching the fiber diameter range of adult murine skeletal muscle, which approximately spans from 10 to 100 μm [88].

The MagneTissue bioreactor system has been thoroughly evaluated in a 3D myogenic model, but is not just limited to muscle tissue engineering purposes. The versatile usage of different strain parameters, e.g. static, cyclic, ramp or a combination thereof, could be used to create *in vitro* muscle disease models related to sarcopenia, trauma and/or exercise-induced damage. Besides, other tissues in the human body such as tendons and ligaments are also highly influenced by mechanotransduction and may serve as additional application fields of the bioreactor. As future plans, we aim to develop vascularization strategies to facilitate nutrient and oxygen supply within the constructs. Another essential interest is to investigate the role of mechanotransduction and which mechanosensitive signaling pathways contribute to myogenic differentiation, which would help to gain greater insight into the spatiotemporal provision of distinct mechanical stimuli. Elucidating optimized strain patterns will be dependent on this knowledge and improve the performance of tissue engineered muscle by modulating these essential signaling pathways.

Funding

This study was supported by the City of Vienna Competence Team reacTissue Project (MA27 Grant 12-06) and the European Union 7th Framework Programme (Biodesign: #262948).

Acknowledgements

We would like to thank Melanie Schöllhorn for the preliminary work and test set-up of the bioreactor and Terje "TJ" Wimberger

for assisting in analysis of immunofluorescence data. We would also like to thank Monika Debreczeny (BOKU, Vienna, Austria) for technical assistance in confocal microscopy. We are particularly thankful for the critical input and comments of Peter Zammit and Nicolas Figeac (Kings College, London, United Kingdom) on our work as LBI Trauma and UAS Technikum Wien cooperation partners within Biodesign. We are indebted to the congenial minds of Zafar Khakpour (LBI Trauma, Vienna, Austria), Dominik Hanetseder, Daniel Faust, Ewald Schmudermayer (UAS Technikum Wien, Vienna, Austria), Andreas Graupe and Johannes Schachner (TGM, Vienna, Austria) for designing, optimizing and building the MagneTissue bioreactor and programming the software.

References

[1] I. Janssen, S.B. Heymsfield, Z.M. Wang, R. Ross, Skeletal muscle mass and distribution in 468 men and women aged 18–88 yr, J. Appl. Physiol. 2000 (89) (1985) 81–88.
[2] L. Baoge, E. Van Den Steen, S. Rimbaut, N. Philips, E. Witvrouw, K.F. Almqvist, et al., Treatment of skeletal muscle injury: a review, ISRN Orthopedics 2012 (2012) 689012.
[3] M. Koning, M.C. Harmsen, M.J. van Luyn, P.M. Werker, Current opportunities and challenges in skeletal muscle tissue engineering, J. Tissue Eng. Regen. Med. 3 (2009) 407–415.
[4] W. Bian, N. Bursac, Tissue engineering of functional skeletal muscle: challenges and recent advances, IEEE Eng. Med. Biol. Mag. 27 (2008) 109–113.
[5] G. Cittadella Vigodarzere, S. Mantero, Skeletal muscle tissue engineering: strategies for volumetric constructs, Front. Physiol. 5 (2014) 362.
[6] H.H. Vandenburgh, P. Karlisch, Longitudinal growth of skeletal myotubes in vitro in a new horizontal mechanical cell stimulator, In Vitro Cell. Dev. Biol.: J. Tissue Cult. Assoc. 25 (1989) 607–616.
[7] H.H. Vandenburgh, P. Karlisch, L. Farr, Maintenance of highly contractile tissue-cultured avian skeletal myotubes in collagen gel, In Vitro Cell. Dev. Biol.: J. Tissue Cult. Assoc. 24 (1988) 166–174.
[8] W. Bian, N. Bursac, Engineered skeletal muscle tissue networks with controllable architecture, Biomaterials 30 (2009) 1401–1412.
[9] U. Cheema, S.Y. Yang, V. Mudera, G.G. Goldspink, R.A. Brown, 3-D in vitro model of early skeletal muscle development, Cell Motil. Cytoskelet. 54 (2003) 226–236.
[10] Y.C. Huang, R.G. Dennis, L. Larkin, K. Baar, Rapid formation of functional muscle in vitro using fibrin gels, J. Appl. Physiol. 2005 (98) (1985) 706–713.
[11] T. Matsumoto, J. Sasaki, E. Alsberg, H. Egusa, H. Yatani, T. Sohmura, Three-dimensional cell and tissue patterning in a strained fibrin gel system, PLoS ONE 2 (2007) e1211.
[12] Y. Morimoto, M. Kato-Negishi, H. Onoe, S. Takeuchi, Three-dimensional neuron-muscle constructs with neuromuscular junctions, Biomaterials 34 (2013) 9413–9419.
[13] T. Okano, T. Matsuda, Tissue engineered skeletal muscle: preparation of highly dense, highly oriented hybrid muscular tissues, Cell Transplant. 7 (1998) 71–82.
[14] D.W. van der Schaft, A.C. van Spreeuwel, H.C. van Assen, F.P. Baaijens, Mechanoregulation of vascularization in aligned tissue-engineered muscle: a role for vascular endothelial growth factor, Tissue Eng. A 17 (2011) 2857–2865.
[15] C.L. Chiu, V. Hecht, H. Duong, B. Wu, B. Tawil, Permeability of three-dimensional fibrin constructs corresponds to fibrinogen and thrombin concentrations, BioRes. Open Access 1 (2012) 34–40.
[16] S.L. Rowe, S. Lee, J.P. Stegemann, Influence of thrombin concentration on the mechanical and morphological properties of cell-seeded fibrin hydrogels, Acta Biomater. 3 (2007) 59–67.
[17] A. Undas, R.A. Ariens, Fibrin clot structure and function: a role in the pathophysiology of arterial and venous thromboembolic diseases, Arterioscler. Thromb. Vasc. Biol. 31 (2011) e88–e99.
[18] M. Buckingham, How the community effect orchestrates muscle differentiation, BioEssays 25 (2003) 13–16.
[19] N.R. Martin, S.L. Passey, D.J. Player, A. Khodabukus, R.A. Ferguson, A.P. Sharples, et al., Factors affecting the structure and maturation of human tissue engineered skeletal muscle, Biomaterials 34 (2013) 5759–5765.
[20] A. Sahni, C.W. Francis, Vascular endothelial growth factor binds to fibrinogen and fibrin and stimulates endothelial cell proliferation, Blood 96 (2000) 3772–3778.
[21] A. Sahni, O.D. Altland, C.W. Francis, FGF-2 but not FGF-1 binds fibrin and supports prolonged endothelial cell growth, J. Thromb. Haemost. 1 (2003) 1304–1310.
[22] A. Sahni, T. Odrljin, C.W. Francis, Binding of basic fibroblast growth factor to fibrinogen and fibrin, J. Biol. Chem. 273 (1998) 7554–7559.
[23] P.G. Campbell, S.K. Durham, J.D. Hayes, A. Suwanichkul, D.R. Powell, Insulin-like growth factor-binding protein-3 binds fibrinogen and fibrin, J. Biol. Chem. 274 (1999) 30215–30221.
[24] R.L. Lieber, J. Friden, Functional and clinical significance of skeletal muscle architecture, Muscle Nerve 23 (2000) 1647–1666.
[25] H. Huxley, J. Hanson, Changes in the cross-striations of muscle during contraction and stretch and their structural interpretation, Nature 173 (1954) 973–976.
[26] T.J. Burkholder, Mechanotransduction in skeletal muscle, Front. Biosci. 12 (2007) 174–191.
[27] C.A. Powell, B.L. Smiley, J. Mills, H.H. Vandenburgh, Mechanical stimulation improves tissue-engineered human skeletal muscle, Am. J. Physiol. Cell Physiol. 283 (2002) C1557–C1565.
[28] N.A. Taylor, J.G. Wilkinson, Exercise-induced skeletal muscle growth. Hypertrophy or hyperplasia?, Sports Med 3 (1986) 190–200.
[29] P.J. Atherton, N.J. Szewczyk, A. Selby, D. Rankin, K. Hillier, K. Smith, et al., Cyclic stretch reduces myofibrillar protein synthesis despite increases in FAK and anabolic signalling in L6 cells, J. Physiol. 587 (2009) 3719–3727.
[30] S.H. Kook, H.J. Lee, W.T. Chung, I.H. Hwang, S.A. Lee, B.S. Kim, et al., Cyclic mechanical stretch stimulates the proliferation of C2C12 myoblasts and inhibits their differentiation via prolonged activation of p38 MAPK, Mol. Cells 25 (2008) 479–486.
[31] A. Kumar, R. Murphy, P. Robinson, L. Wei, A.M. Boriek, Cyclic mechanical strain inhibits skeletal myogenesis through activation of focal adhesion kinase, Rac-1 GTPase, and NF-kappaB transcription factor, FASEB J. 18 (2004) 1524–1535.
[32] G. Moon du, G. Christ, J.D. Stitzel, A. Atala, J.J. Yoo, Cyclic mechanical preconditioning improves engineered muscle contraction, Tissue Eng. A 14 (2008) 473–482.
[33] V. Hosseini, S. Ahadian, S. Ostrovidov, G. Camci-Unal, S. Chen, H. Kaji, et al., Engineered contractile skeletal muscle tissue on a microgrooved methacrylated gelatin substrate, Tissue Eng. A 18 (2012) 2453–2465.
[34] M.T. Lam, Y.C. Huang, R.K. Birla, S. Takayama, Microfeature guided skeletal muscle tissue engineering for highly organized 3-dimensional free-standing constructs, Biomaterials 30 (2009) 1150–1155.
[35] R. Shah, J.C. Knowles, N.P. Hunt, M.P. Lewis, Development of a novel smart scaffold for human skeletal muscle regeneration, J. Tissue Eng. Regen. Med. (2013).
[36] R.G. Dennis, P.E. Kosnik 2nd, Excitability and isometric contractile properties of mammalian skeletal muscle constructs engineered in vitro, In Vitro Cell. Dev. Biol. Anim. 36 (2000) 327–335.
[37] H. Fujita, T. Nedachi, M. Kanzaki, Accelerated de novo sarcomere assembly by electric pulse stimulation in C2C12 myotubes, Exp. Cell Res. 313 (2007) 1853–1865.
[38] M.L. Langelaan, K.J. Boonen, K.Y. Rosaria-Chak, D.W. van der Schaft, M.J. Post, F.P. Baaijens, Advanced maturation by electrical stimulation: differences in response between C2C12 and primary muscle progenitor cells, J. Tissue Eng. Regen. Med. 5 (2011) 529–539.
[39] K. Nagamine, T. Kawashima, T. Ishibashi, H. Kaji, M. Kanzaki, M. Nishizawa, Micropatterning contractile C2C12 myotubes embedded in a fibrin gel, Biotechnol. Bioeng. 105 (2010) 1161–1167.
[40] A.S. Smith, S. Passey, L. Greensmith, V. Mudera, M.P. Lewis, Characterization and optimization of a simple, repeatable system for the long term in vitro culture of aligned myotubes in 3D, J. Cell. Biochem. 113 (2012) 1044–1053.
[41] B.T. Corona, M.A. Machingal, T. Criswell, M. Vadhavkar, A.C. Dannahower, C. Bergman, et al., Further development of a tissue engineered muscle repair construct in vitro for enhanced functional recovery following implantation in vivo in a murine model of volumetric muscle loss injury, Tissue Eng. A 18 (2012) 1213–1228.
[42] J. Schindelin, I. Arganda-Carreras, E. Frise, V. Kaynig, M. Longair, T. Pietzsch, et al., Fiji: an open-source platform for biological-image analysis, Nat. Methods 9 (2012) 676–682.
[43] A.J. Engler, S. Sen, H.L. Sweeney, D.E. Discher, Matrix elasticity directs stem cell lineage specification, Cell 126 (2006) 677–689.
[44] Y. Capetanaki, D.J. Milner, G. Weitzer, Desmin in muscle formation and maintenance: knockouts and consequences, Cell Struct. Funct. 22 (1997) 103–116.
[45] M.L. Costa, R. Escaleira, A. Cataldo, F. Oliveira, C.S. Mermelstein, Desmin: molecular interactions and putative functions of the muscle intermediate filament protein, Braz. J. Med. Biol. Res. 37 (2004) 1819–1830.
[46] H. Aubin, J.W. Nichol, C.B. Hutson, H. Bae, A.L. Sieminski, D.M. Cropek, et al., Directed 3D cell alignment and elongation in microengineered hydrogels, Biomaterials 31 (2010) 6941–6951.
[47] A.J. Engler, M.A. Griffin, S. Sen, C.G. Bonnemann, H.L. Sweeney, D.E. Discher, Myotubes differentiate optimally on substrates with tissue-like stiffness: pathological implications for soft or stiff microenvironments, J. Cell Biol. 166 (2004) 877–887.
[48] J.P. Hyatt, G.E. McCall, E.M. Kander, H. Zhong, R.R. Roy, K.A. Huey, PAX3/7 expression coincides with MyoD during chronic skeletal muscle overload, Muscle Nerve 38 (2008) 861–866.
[49] P.S. Zammit, F. Relaix, Y. Nagata, A.P. Ruiz, C.A. Collins, T.A. Partridge, et al., Pax7 and myogenic progression in skeletal muscle satellite cells, J. Cell Sci. 119 (2006) 1824–1832.
[50] F. Relaix, D. Montarras, S. Zaffran, B. Gayraud-Morel, D. Rocancourt, S. Tajbakhsh, et al., Pax3 and Pax7 have distinct and overlapping functions in adult muscle progenitor cells, J. Cell Biol. 172 (2006) 91–102.
[51] H.C. Olguin, B.B. Olwin, Pax-7 up-regulation inhibits myogenesis and cell cycle progression in satellite cells: a potential mechanism for self-renewal, Dev. Biol. 275 (2004) 375–388.

Please cite this article in press as: P. Heher et al., A novel bioreactor for the generation of highly aligned 3D skeletal muscle-like constructs through orientation of fibrin via application of static strain, Acta Biomater. (2015), http://dx.doi.org/10.1016/j.actbio.2015.06.033

[52] M.A. Rudnicki, P.N. Schnegelsberg, R.H. Stead, T. Braun, H.H. Arnold, R. Jaenisch, MyoD or Myf-5 is required for the formation of skeletal muscle, Cell 75 (1993) 1351–1359.
[53] S. Yokoyama, H. Asahara, The myogenic transcriptional network, Cell. Mol. Life Sci. 68 (2011) 1843–1849.
[54] C.A. Collins, V.F. Gnocchi, R.B. White, L. Boldrin, A. Perez-Ruiz, F. Relaix, et al., Integrated functions of Pax3 and Pax7 in the regulation of proliferation, cell size and myogenic differentiation, PLoS ONE 4 (2009) e4475.
[55] P. Londhe, J.K. Davie, Sequential association of myogenic regulatory factors and E proteins at muscle-specific genes, Skelet. Muscle 1 (2011) 14.
[56] X. Wang, Q.Q. Huang, M.T. Breckenridge, A. Chen, T.O. Crawford, D.H. Morton, et al., Cellular fate of truncated slow skeletal muscle troponin T produced by Glu180 nonsense mutation in amish nemaline myopathy, J. Biol. Chem. 280 (2005) 13241–13249.
[57] B. Wei, J.P. Jin, Troponin T isoforms and posttranscriptional modifications: evolution, regulation and function, Arch. Biochem. Biophys. 505 (2011) 144–154.
[58] A. Khodabukus, K. Baar, Regulating fibrinolysis to engineer skeletal muscle from the C2C12 cell line, Tissue Eng. C, Methods 15 (2009) 501–511.
[59] H.H. Vandenburgh, Cell shape and growth regulation in skeletal muscle: exogenous versus endogenous factors, J. Cell. Physiol. 116 (1983) 363–371.
[60] P. Bajaj, B. Reddy Jr., L. Millet, C. Wei, P. Zorlutuna, G. Bao, et al., Patterning the differentiation of C2C12 skeletal myoblasts, Integr. Biol. (Camb.) 3 (2011) 897–909.
[61] S.L. Hume, S.M. Hoyt, J.S. Walker, B.V. Sridhar, J.F. Ashley, C.N. Bowman, et al., Alignment of multi-layered muscle cells within three-dimensional hydrogel macrochannels, Acta Biomater. 8 (2012) 2193–2202.
[62] K. Donnelly, A. Khodabukus, A. Philp, L. Deldicque, R.G. Dennis, K. Baar, A novel bioreactor for stimulating skeletal muscle in vitro, Tissue Eng. C, Methods 16 (2010) 711–718.
[63] M. Zhan, B. Jin, S.E. Chen, J.M. Reecy, Y.P. Li, TACE release of TNF-alpha mediates mechanotransduction-induced activation of p38 MAPK and myogenesis, J. Cell Sci. 120 (2007) 692–701.
[64] G. Candiani, S.A. Riboldi, N. Sadr, S. Lorenzoni, P. Neuenschwander, F.M. Montevecchi, et al., Cyclic mechanical stimulation favors myosin heavy chain accumulation in engineered skeletal muscle constructs, J. Appl. Biomater. Biomech. 8 (2010) 68–75.
[65] I.C. Liao, J.B. Liu, N. Bursac, K.W. Leong, Effect of electromechanical stimulation on the maturation of myotubes on aligned electrospun fibers, Cell. Mol. Bioeng. 1 (2008) 133–145.
[66] H.H. Vandenburgh, S. Swasdison, P. Karlisch, Computer-aided mechanogenesis of skeletal muscle organs from single cells in vitro, FASEB J. 5 (1991) 2860–2867.
[67] S. Rangarajan, L. Madden, N. Bursac, Use of flow, electrical, and mechanical stimulation to promote engineering of striated muscles, Ann. Biomed. Eng. 42 (2014) 1391–1405.
[68] K.J. Boonen, M.L. Langelaan, R.B. Polak, D.W. van der Schaft, F.P. Baaijens, M.J. Post, Effects of a combined mechanical stimulation protocol: value for skeletal muscle tissue engineering, J. Biomech. 43 (2010) 1514–1521.
[69] M. Liu, S. Montazeri, T. Jedlovsky, R. Van Wert, J. Zhang, R.K. Li, et al., Bio-stretch, a computerized cell strain apparatus for three-dimensional organotypic cultures, In Vitro Cell. Dev. Biol. Anim. 35 (1999) 87–93.
[70] A. Auluck, V. Mudera, N.P. Hunt, M.P. Lewis, A three-dimensional in vitro model system to study the adaptation of craniofacial skeletal muscle following mechanostimulation, Eur. J. Oral Sci. 113 (2005) 218–224.
[71] M.W. Mosesson, Fibrinogen and fibrin structure and functions, J. Thromb. Haemost. 3 (2005) 1894–1904.
[72] J.W. Weisel, R.I. Litvinov, Mechanisms of fibrin polymerization and clinical implications, Blood 121 (2013) 1712–1719.
[73] A.M. Collinsworth, S. Zhang, W.E. Kraus, G.A. Truskey, Apparent elastic modulus and hysteresis of skeletal muscle cells throughout differentiation, Am. J. Physiol. Cell Physiol. 283 (2002) C1219–C1227.
[74] A. Gugerell, K. Schossleitner, S. Wolbank, S. Nurnberger, H. Redl, H. Gulle, et al., High thrombin concentrations in fibrin sealants induce apoptosis in human keratinocytes, J. Biomed. Mater. Res. A 100 (2012) 1239–1247.
[75] D. Stewart, The Role of Tension in Muscle Growth, Academic Press, Inc., New York, 1972.
[76] C.F. Bentzinger, Y.X. Wang, M.A. Rudnicki, Building muscle: molecular regulation of myogenesis, Cold Spring Harb. Perspect. Biol. (2012) 4.
[77] P. Seale, L.A. Sabourin, A. Girgis-Gabardo, A. Mansouri, P. Gruss, M.A. Rudnicki, Pax7 is required for the specification of myogenic satellite cells, Cell 102 (2000) 777–786.
[78] J.E. Morgan, T.A. Partridge, Muscle satellite cells, Int. J. Biochem. Cell Biol. 35 (2003) 1151–1156.
[79] N. Figeac, O. Serralbo, C. Marcelle, P.S. Zammit, ErbB3 binding protein-1 (Ebp1) controls proliferation and myogenic differentiation of muscle stem cells, Dev. Biol. 386 (2014) 135–151.
[80] F. Relaix, P.S. Zammit, Satellite cells are essential for skeletal muscle regeneration: the cell on the edge returns centre stage, Development 139 (2012) 2845–2856.
[81] P. Zhang, X. Liang, T. Shan, Q. Jiang, C. Deng, R. Zheng, et al., MTOR is necessary for proper satellite cell activity and skeletal muscle regeneration, Biochem. Biophys. Res. Commun (2015).
[82] M. Vandromme, C. Chailleux, F. Escaffit, D. Trouche, Binding of the retinoblastoma protein is not the determinant for stable repression of some E2F-regulated promoters in muscle cells, Mol. Cancer Res. 6 (2008) 418–425.
[83] N. Murata, S. Ito, K. Furuya, N. Takahara, K. Naruse, H. Aso, et al., Ca2+ influx and ATP release mediated by mechanical stretch in human lung fibroblasts, Biochem. Biophys. Res. Commun. 453 (2014) 101–105.
[84] S. Ito, B. Suki, H. Kume, Y. Numaguchi, M. Ishii, M. Iwaki, et al., Actin cytoskeleton regulates stretch-activated Ca2+ influx in human pulmonary microvascular endothelial cells, Am. J. Respir. Cell Mol. Biol. 43 (2010) 26–34.
[85] C. Zobel, O.R. Rana, E. Saygili, B. Bolck, H. Diedrichs, H. Reuter, et al., Mechanisms of Ca2+-dependent calcineurin activation in mechanical stretch-induced hypertrophy, Cardiology 107 (2007) 281–290.
[86] Y. Takayama, A. Wagatsuma, T. Hoshino, K. Mabuchi, Simple micropatterning method for enhancing fusion efficiency and responsiveness to electrical stimulation of C2C12 myotubes, Biotechnol. Prog. 31 (2015) 220–225.
[87] H.H. Vandenburgh, Motion into mass: how does tension stimulate muscle growth?, Med Sci. Sports Exerc. 19 (1987) S142–S149.
[88] P.V. Hegarty, A.C. Hooper, Sarcomere length and fibre diameter distributions in four different mouse skeletal muscles, J. Anat. 110 (1971) 249–257.

Please cite this article in press as: P. Heher et al., A novel bioreactor for the generation of highly aligned 3D skeletal muscle-like constructs through orientation of fibrin via application of static strain, Acta Biomater. (2015), http://dx.doi.org/10.1016/j.actbio.2015.06.033